Target Tracking via Recursive Bayesian State Estimation in Cognitive Radar Networks[☆]

Yijian Xiang[a], Murat Akcakaya[b], Satyabrata Sen[c], Deniz Erdogmus[d], Arye Nehorai[a,*]

[a]*Washington University in St. Louis, St. Louis, MO 63130 USA*
[b]*University of Pittsburgh, Pittsburgh, PA 15213 USA*
[c]*Oak Ridge National Laboratory, Oak Ridge, TN 37831 USA*
[d]*Northeastern University, Boston, MA 02115 USA*

Abstract

To cope with complicated environments and stealthier targets, incorporating intelligence and cognition cycles into target tracking is of great importance in modern sensor network management. With remarkable advances in sensor techniques and deployable platforms, a sensing system has freedom to select a subset of available radars, plan their trajectories, and transmit designed waveforms. In this paper, we propose a general framework for single target tracking in cognitive networks of radars, including consideration of waveform design, path planning, and radar selection, which are separately but not jointly taken into account in existing work. The tracking procedure, built on the theories of dynamic graphical models (DGM) and recursive Bayesian state estimation (RBSE), is formulated as two iterative steps: (i) solving a combinatorial optimization problem to select the optimal subset of radars, waveforms, and locations for the next tracking instant, and (ii) acquiring the recursive Bayesian state estimation to accurately track the target. Further, an illustrative example introduces a specific scenario in 2-D space. Simulation results based on the scenario demonstrate that the proposed framework can accurately track the target under the management of the network of radars.

Keywords: Recursive Bayesian state estimation, waveform design, path planning, sensor selection, target tracking, network of radars.

1. Introduction

Target tracking has long been one of the most relevant and challenging problems in a wide variety of military and civilian radar systems. The primary objective of a conventional tracking system is to provide accurate estimates of

[☆]The work was supported by AFOSR under Grant No. FA9550-16-1-0386. The work of Sen was performed at the Oak Ridge National Laboratory, managed by UT-Battelle, LLC, for the U.S. Department of Energy, under Contract DE-AC05-00OR22725. The United States Government retains and the publisher, by accepting the article for publication, acknowledges that the United States Government retains a nonexclusive, paid-up, irrevocable, world-wide license to publish or reproduce the published form of this manuscript, or allow others to do so, for United States Government purposes. The Department of Energy will provide public access to these results of federally sponsored research in accordance with the DOE Public Access Plan (http://energy.gov/downloads/doe-public-access-plan).

[*]Corresponding author

Email addresses: yijian.xiang@wustl.edu (Yijian Xiang), akcakaya@pitt.edu (Murat Akcakaya), sens@ornl.gov (Satyabrata Sen), erdogmus@ece.neu.edu (Deniz Erdogmus), nehorai@ese.wustl.edu (Arye Nehorai)

an unknown target's state, e.g., its position and velocity. This can be done in a time-sequential manner by utilizing the received radar measurements and assumed target kinematic models. However, in modern tracking scenarios, it has become imperative to augment such stand-alone trackers with various intelligent and cognitive support-modules in order to successfully meet performance criteria [1–3]. Nowadays, the targets have become stealthier and more agile, and the tracking environments have become more complicated, involving numerous shadow regions due to the lack of line-of-sight propagation paths. In response, radar systems have evolved to include multiple static or mobile platforms that coordinate among themselves to improve the tracking accuracy. For example, tracking targets in urban environments using a fleet of self-controlled and self-tasked unmanned aerial vehicles (UAVs) is much more prevalent now than it was a few years ago.

To improve tracking performance in such complicated scenarios, a system of radars has to fully extract and utilize the environmental information, and intelligently manage its sensor (individual radars) resources. Therefore, in addition to using standard tracking filters, the radar system has to incorporate three key techniques: (i) *waveform design*, to extract more target information by adaptively designing transmitted signals, (ii) *path planning*, to obtain better "looks" at the target by actively adjusting the target-radar geometry, and (iii) *sensor selection*, to optimally select a subset of radars that can track targets with satisfactory performance. In this paper, we develop a target tracking framework that enables simultaneous sensor subset selection, waveform design, and path planning to build a sophisticated tracking system.

1.1. Related Work

A few works in the literature adopt one or combine two of the above three techniques in target tracking; however, no other work thus far has simultaneously applied waveform-agile sensing, planned the corresponding paths, and intelligently selected the subset of radars. For example, dynamic waveform adaption has been extensively investigated in target detection [4–10] and tracking [11–24] to meet a radar's constantly changing requirements for the target information. The motivation behind the adaptive waveform design techniques is to gain better tracking performance by integrating the radar transmitter and receiver in a closed-loop fashion. Previous works focus on analyzing the output of a matched filter and on improving the resolution [25] by treating the radar and tracker as independent subsystems [26]. In recent works, as the tracker recursively estimates the target state, the radar transmitter is adapted to design the next transmitted waveform according to a predefined utility function, such as the mean-square tracking error [15, 16], the trace of the posterior Cramér-Rao lower bound (PCRLB) [11, 27], and the mutual information [12, 28, 29]. In general, the utility function provides one-step ahead design (i.e., greedy); only a few articles discuss multi-step ahead waveform selection [15, 30]. Some works directly design the frequency spectrum of the waveform by using optimal frequencies [4, 5, 31], while others select the waveform from a parameterized waveform library [29], such as a linear frequency-modulated (LFM) library [11]. Besides, waveform design for multistatic target tracking is also investigated [32]. Although waveform design and scheduling applications show promising results, they face challenges in selecting proper design metrics, designing optimal or nearly-optimal waveform families with respect to

these criteria, and formulating computationally tractable scheduling policies [33].

Path planning is another important and fundamental issue for radars, particularly for those which are installed on moving platforms, such as UAVs. To improve the performance of target localization and tracking, careful design of radar paths to actively steer them to the optimal places within the kinematic capabilities [34–39] provides another degree of freedom in utilizing the feedback information from receivers. A simple case of obtaining the optimal trajectory of a single radar by maximizing the determinant of the Fisher information matrix in a passive bearings-only case for fixed target localization is introduced in [36]. Multiple radars cases are considered in [34, 35, 37–39], and cooperative path planning strategies are derived for both passive and active radars. However, in general, it is extremely complicated to plan the paths of multiple radars simultaneously under certain kinematic constraints while appropriately adopting non-myopic policies.

Sensor selection and resource allocation schemes are generally employed in sensor network management problems to intelligently assign a subset of sensors to accomplish the task with satisfactory performance or minimized usage of resources. A sensor selection problem is usually a combinatorial optimization problem, which can be NP hard to solve for the optimal solution, and therefore approximate techniques are necessary to search for an acceptable solution. In the literature, the sensor selection problem is usually cast in one of three ways. It can be formulated as a convex optimization problem with a heuristic searching method [40], as the maximization of a submodular function problem (which can be solved by a greedy algorithm with guaranteed performance) [41], or as a linear programming and a semi-definite programming (SDP) problem by respectively considering the measurement noises to be uncorrelated and correlated [42]. In regard to target tracking, the sensor selection and resource allocation schemes are adaptively applied from time to time [42–49].

In addition, a few works combine two of the three techniques (waveform design, path planning, and sensor selection) to further improve the tracking performance or decrease the resource usage. For example, waveform design and path planning are jointly considered in [24] and [50]. In [24], adaptive selection of the optimal pulse repetition interval (PRI) from a set of allowed values, and optimization of the radar trajectory using the trace of weighted PCRLB, are proposed, whereas [50] jointly optimizes the waveform parameters of Gaussian-LFM pulses and the guiding commands of multistatic radars using the trace of the PCRLB. Although multiple radars are taken into account, no subset selection strategy is adopted in [50], implying that the radars use all the available resources to track the target, which may lead to a waste of resources. In [51, 52], waveform design and sensor selection are combined for static radars to select adaptive waveforms and a subset of sensors in accordance with the resource constraints. In our previous work [53], we proposed a framework of single target tracking based on the theories of DGM and RBSE, jointly considering radar selection and path planning. However, the advantages of the waveform-agility were not exploited to further improve the tracking performance and system intelligence.

1.2. Our Contributions

In this paper, we propose a target tracking framework that simultaneously designs the transmit waveform, plans the radar trajectory, and selects the appropriate radar subset. Building on the established theories of dynamic graphical models (DGM) and recursive Bayesian state estimation (RBSE) [54, 55], we choose the expected cross-entropy as the objective function and solve a combinatorial optimization problem to select the optimal subset of radars that transmit well-designed waveforms from their best locations for receiving the most informative measurements during the next tracking instant. The received measurements associated with history information are then processed by a tracker to achieve a more accurate target state estimation. Additionally, we validate the proposed framework by constructing an illustrative case, where radars with certain moving constraints track a single target in a 2-D space. Specifically, we choose this simplified case as it is a representation of a large-scale network of cognitive radars which have certain constraints about coverage area and path. As we describe later in Section 3, these constraints reflect real-time scenarios especially when each radar in the network is aware of the locations of the other radars in the network and when overlapping of coverage area among the radars along same path are avoided using the location information assuming that the target is in the far-field compared to all the radars in the network. Finally, simulation results are given to show the feasibility of the framework. The sensing system of the sensor network can achieve satisfying tracking performance with relatively low process noise.

Our main contribution in this paper is to consider the path design, waveform design and radar subset selection simultaneously in target tracking with a large-scale of network of radars. As we show with the numerical examples, under certain assumptions our method is computationally feasible and our approach is an important step towards the realization of a network of cognitive radars in real-time for target tracking. Even though the concept of cognitive radar has been proposed more than a decade ago [1], until now a real-time implementation of a cognitive radar has not been presented. The rest of paper is organized as follows. In Section 2, we present our framework for jointly selecting the subset of sensors and the corresponding waveforms with moving radars in target tracking. In Section 3, we give an illustrative example and solve the example based on the proposed framework. Further, experimental results are shown to validate the proposed method. Finally, in Section 4, the paper is concluded and future work is discussed.

2. Framework of Target Tracking in Network of Radars

Our proposed framework formulates the sensor (radar) network management for single target tracking as a combinatorial optimization problem. By solving the combinatorial optimization problem, we choose the optimal subset of radars to transmit well-designed waveforms in the best locations in order to receive the most informative echos in the next tracking step. The echos are then processed by the tracker associated with history information to achieve a reasonable state estimation. Fig. 1 depicts our proposed framework of single target tracking in cognitive network of radars based on a DGM. Without loss of generality, similar to most target tracking application, order-1 Markov processes with finite-dimensional state vectors are considered. The notations of variables of interest and their dependence

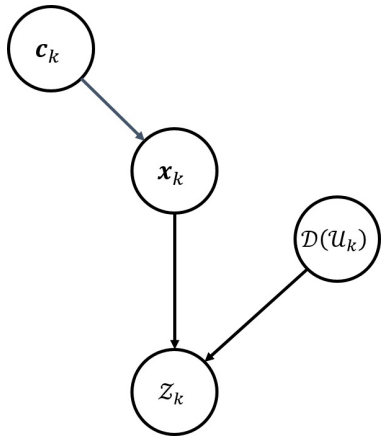

Figure 1: Graphical model (step k). The evolution of the state $\boldsymbol{x}_k$ is dependent on the contextual evidence $\boldsymbol{c}_k$. Here $\mathcal{D}(\mathcal{U}_k)$ indicates the selected radars, the transmitted waveforms, and the radar states; $\mathcal{Z}_k$ denotes noisy measurements of the state $\boldsymbol{x}_k$ if $\mathcal{D}(\mathcal{U}_k)$ is applied.

relationships at time k are defined as follows:

1. The state of the target is denoted as $\boldsymbol{x}_k$, which needs to be estimated from the noisy measurement and contextual information. The state of $\boldsymbol{x}_k$ usually includes the target's current location and velocity. It can be augmented to contain more variables, such as the acceleration of the target and the radar cross section (RCS) of the echos.
2. The target kinematic model, the history information provided by previous measurements, and the statistical environment model are represented as probabilistic contextual evidence, $\boldsymbol{c}_k$.
3. A set (dictionary) is denoted as $\mathcal{D} = \{(\mathcal{D}^s, \mathcal{D}^w, \mathcal{D}^p)\}$, where $\mathcal{D}^s$ contains all the possible radars that can be managed in the network, $\mathcal{D}^w$ contains all the possible waveforms that can be transmitted by the radars, and $\mathcal{D}^p$ includes all the states of radars (e.g., positions and velocities) that can be achieved.
4. A set of indices is denoted as $\mathcal{U}_k = \{(\mathcal{U}_k^s, \mathcal{U}_k^w, \mathcal{U}_k^p)\}$, where $\mathcal{U}_k^s$ denotes the set of radars that are selected to transmit the corresponding waveforms represented by the index set $\mathcal{U}_k^w$ with their states indicated by $\mathcal{U}_k^p$ at time step k.
5. The measurements at time k that are collected by the subset of radars with certain waveforms and states suggested by $\mathcal{D}(\mathcal{U}_k)$ are denoted as $\mathcal{Z}_k = \{z_k^{(i)} | i \in \mathcal{U}_k^s\}$, where $z_k^{(i)}$ is the measurement of i_{th} radar.

The probabilistic contextual evidence $\boldsymbol{c}_k$ could include any information that might affect the estimation of the target state. It could involve several kinematic models to describe the possible motion modes of the target. A commonly used type of contextual evidence is previously collected measurements, which influence the state via estimations of previous states. Further, the contextual evidence also could be provided by a pre-trained environment model in the workspace. For instance, the sensing system has an environment model describing the distribution of obstacles, and prior knowledge that the target tends to avoid obstacles rather than strike them. In this paper, we use only one kinematic model together with previous measurements as the probabilistic contextual evidence $\boldsymbol{c}_k$. In order to further

describe the framework in detail, we define the signal model, kinematic model, measurement model, and recursive Bayesian estimation technique in the following subsections.

2.1. Signal Model

The narrowband waveform of the transmitted signal of the i_{th} radar has the following form,

$$g^{(i)}(t) = s^{(i)}(t)e^{j2\pi f_c^{(i)}t}, \tag{1}$$

where $s^{(i)}(t)$ is the complex envelope of the signal, and $f_c^{(i)}$ is the carrier frequency. The corresponding echo from the target in the baseband is

$$r^{(i)}(t) = \alpha(f^{(i)})s^{(i)}(t-\tau^{(i)})e^{j2\pi\nu^{(i)}(t-\tau^{(i)})}e^{-j2\pi f_c^{(i)}\tau^{(i)}} + n^{(i)}(t), \tag{2}$$

where $\tau^{(i)}$ is the time delay, $\nu^{(i)}$ is the Doppler frequency, $n^{(i)}(t)$ is the complex Gaussian noise, $f^{(i)}$ is the frequency that i_{th} radar transmits after frequency modulation, and $\alpha(f^{(i)})$ is the complex reflectivity caused by the radar cross section (RCS) of the target and phase shift. Note that here we assume that the complex reflectivity is a function of the frequency that the radar transmits. Note that if we consider the scenario in a 2-D space, we have

$$\tau^{(i)} = \frac{2\sqrt{(x-x^{(i)})^2 + (y-y^{(i)})^2}}{c}, \tag{3}$$

$$\nu^{(i)} = -\frac{2f_c^{(i)}}{c}\frac{(\dot{x}-\dot{x}^{(i)})(x-x^{(i)}) + (\dot{y}-\dot{y}^{(i)})(y-y^{(i)})}{\sqrt{(x-x^{(i)})^2 + (y-y^{(i)})^2}}, \tag{4}$$

where c is the speed of light, (x, y) is the position of the target, $(x^{(i)}, y^{(i)})$ is the position of the i_{th} radar, $(\dot{x}, \dot{y})$ is the velocity of the target, and $(\dot{x}^{(i)}, \dot{y}^{(i)})$ is the velocity of the i_{th} radar. The above formulas can be easily extended to the case of 3-D space.

Here we give a specific example of the signal models used by a network of radars. Assuming that all the radars in the network share the same carrier frequency f_c, and we let

$$s^{(i)}(t) = u(t)e^{j2\pi f_\xi^{(i)}t}, \tag{5}$$

where $u(t)$ can be a square pulse which is shared by all the radars, and the waveform agility is dependent on the frequency $f_\xi^{(i)}$ that is modulated by each radar separately. Note that the modulated frequency $f_\xi^{(i)}$ is chosen from a library $\{f_{\xi,1}, \ldots, f_{\xi,W}\}$, which contains different discrete frequencies designed in advance. The range resolution is determined by the bandwidth of $u(t)$, thus leading to the same range resolution for each radar even though different waveforms could be transmitted. In this case, the complex reflectivity $\alpha(\cdot)$ of the echo in Eqn. 2 is a function of the modulated frequency $f_\xi^{(i)}$, i.e., $\alpha(f^{(i)})$ can be denoted as $\alpha(f_\xi^{(i)})$.

2.2. Kinematic Model

The target moving in the surveillance space follows the kinematic model,

$$\boldsymbol{x}_{k+1} = \boldsymbol{f}_k(\boldsymbol{x}_k) + \boldsymbol{v}_k, \tag{6}$$

where k is the time index, $\boldsymbol{x}_k$ is the target state, $\boldsymbol{f}_k(\cdot)$ is the state transition function, and $\boldsymbol{v}_k$ denotes the process noise.

A common example of the kinematic model is the noisy constant velocity (CV) model [56],

$$\boldsymbol{x}_{k+1} = A_k\boldsymbol{x}_k + \boldsymbol{v}_k, \tag{7}$$

where $\boldsymbol{x}_k = [x_k, \dot{x}_k, y_k, \dot{y}_k]^\mathsf{T}$ if a 2-D scenario is considered, (x_k, y_k) and $(\dot{x}_k, \dot{y}_k)$ are the position and velocity of the target at time k, respectively, and the process noise $\boldsymbol{v}_k$ is white Gaussian noise. In addition, the state transition matrix is

$$A_k = I_2 \otimes \bar{A}_k, \tag{8}$$

$$\bar{A}_k = \begin{bmatrix} 1 & T_{\text{in},k} \\ 0 & 1 \end{bmatrix}, \tag{9}$$

where I_2 is the 2×2 identity matrix, $\otimes$ is the Kronecker product, and $T_{\text{in},k}$ is the time interval between two tracking steps. Furthermore, we have that

$$\mathbb{E}(\boldsymbol{v}_k) = \boldsymbol{0}, \tag{10}$$

$$\mathbb{E}(\boldsymbol{v}_k\boldsymbol{v}_j^\mathsf{T}) = V_k\delta_{kj}, \tag{11}$$

where δ_{kj} is the Kronecker delta function, and the noise covariance matrix is

$$V_k = \text{diag}(q_1, q_2) \otimes \begin{bmatrix} \frac{1}{3}T_{\text{in},k}^4 & \frac{1}{2}T_{\text{in},k}^3 \\ \frac{1}{2}T_{\text{in},k}^3 & T_{\text{in},k}^2 \end{bmatrix}, \tag{12}$$

where q_1 and q_2 are the process noise intensities of the x and y directions, respectively.

2.3. Measurement Model

A general measurement model is given by

$$\boldsymbol{z}_k = \boldsymbol{h}_k(\boldsymbol{x}_k; \mathcal{D}(\mathcal{U}_k)) + \boldsymbol{n}_k, \tag{13}$$

where $\boldsymbol{h}_k(\cdot)$ is a nonlinear mapping from the target state $\boldsymbol{x}_k$ to the noiseless measurement, and $\boldsymbol{n}_k$ is the measurement noise. Note that $\boldsymbol{z}_k$ could be the time delay τ, Doppler frequency ν, or other measurements extracted from the echo via signal processing techniques [26]. In addition, it is optional to use the raw discretized received signal as $\boldsymbol{z}_k$ [11]. In practical applications, the choice of $\boldsymbol{z}_k$ is dependent on the channel capacity, computational resources, and requirements of the algorithms. The dimension of $\boldsymbol{z}_k$ is NJ, where N is the dimension of the measurement of a single radar, and J is the total number of selected radars.

In this paper, we take the raw discretized received signal as an example. We assume that the i_{th} radar is selected by the sensing system to operate at time k; i.e., $i \in \mathcal{U}_k^s$. In addition, we denote the i_{th} radar, the corresponding selected waveform, and its state as $D_k^{(i)}$. According to (2) and assuming that the echo from the target is collected by the i_{th} radar, we have

$$r_k^{(i)}(t) = h_k^{(i)}(t, \boldsymbol{x}_k; D_k^{(i)}) + n_k^{(i)}(t), \quad t = t_1, \ldots, t_N, \tag{14}$$

where the measurement noise $n_k^{(i)}(t)$ is white circularly-symmetric complex Gaussian noise, and

$$h_k^{(i)}(t, \boldsymbol{x}_k; D_k^{(i)}) = \alpha(f_k^{(i)}) s_k^{(i)}(t - \tau_k^{(i)}) e^{j2\pi v_k^{(i)}(t-\tau_k^{(i)})} e^{-j2\pi f_c^{(i)} \tau_k^{(i)}}. \tag{15}$$

We lump all the samples together to obtain

$$\begin{aligned} \tilde{\boldsymbol{r}}_k^{(i)} &= \begin{bmatrix} h_k^{(i)}(t_1, \boldsymbol{x}_k; D_k^{(i)}) \\ \vdots \\ h_k^{(i)}(t_N, \boldsymbol{x}_k; D_k^{(i)}) \end{bmatrix} + \begin{bmatrix} n_k^{(i)}(t_1) \\ \vdots \\ n_k^{(i)}(t_N) \end{bmatrix} \\ &= \tilde{\boldsymbol{h}}_k^{(i)}(\boldsymbol{x}_k; D_k^{(i)}) + \tilde{\boldsymbol{n}}_k^{(i)}. \end{aligned} \tag{16}$$

Since many tracking filters prefer a real expression of the measurement model, we further modify (16) to

$$\begin{aligned} \boldsymbol{z}_k^{(i)} = \boldsymbol{r}_k^{(i)} &= \begin{bmatrix} \text{Re}\{\tilde{\boldsymbol{h}}_k^{(i)}(\boldsymbol{x}_k; D_k^{(i)})\} \\ \text{Im}\{\tilde{\boldsymbol{h}}_k^{(i)}(\boldsymbol{x}_k; D_k^{(i)})\} \end{bmatrix} + \begin{bmatrix} \text{Re}\{\tilde{\boldsymbol{n}}_k^{(i)}\} \\ \text{Im}\{\tilde{\boldsymbol{n}}_k^{(i)}\} \end{bmatrix} \\ &= \boldsymbol{h}_k^{(i)}(\boldsymbol{x}_k; D_k^{(i)}) + \boldsymbol{n}_k^{(i)}, \end{aligned} \tag{17}$$

where $\text{Re}\{\cdot\}$ and $\text{Im}\{\cdot\}$ represent the real and imaginary parts of a complex number, respectively. Note that $\boldsymbol{n}_k^{(i)}$ remains Gaussian. By collecting all the $\boldsymbol{z}_k^{(i)}$ into one vector $\boldsymbol{z}_k$, such that $i \in \mathcal{U}_k^s$, we have

$$\begin{aligned} \boldsymbol{z}_k = \text{vec}\mathcal{Z}_k &= \text{vec}\{\boldsymbol{z}_k^{(i)} | i \in \mathcal{U}_k^s\} \\ &= \text{vec}\{\boldsymbol{h}_k^{(i)}(\boldsymbol{x}_k; D_k^{(i)}) + \boldsymbol{n}_k^{(i)} | i \in \mathcal{U}_k^s\} \\ &= \boldsymbol{h}_k(\boldsymbol{x}_k; \mathcal{D}(\mathcal{U}_k)) + \boldsymbol{n}_k, \end{aligned} \tag{18}$$

where the vec operator lumps the elements in a set into a vector. Furthermore, we define the covariance matrix as,

$$\mathbb{E}(\boldsymbol{n}_k \boldsymbol{n}_j^{\mathsf{T}}) = R_k \delta_{kj}. \tag{19}$$

We should note that the measurement model given by (18) assumes the ideal scenario, in which the radars' beams can always cover the target. However, when the beamwidths are narrow or in other practical situations, it is possible that echo received by a selected radar contains only noise when the target is not covered by its beam. For these cases, the actual measurement should be adjusted to $\boldsymbol{h}_k^{(i)}(\boldsymbol{x}_k; D_k^{(i)}) = 0$.

2.4. Recursive Bayesian Estimation

In target tracking, we aim to recursively estimate the posterior distribution

$$p(\boldsymbol{x}_k|\mathcal{Z}_{1:k};\mathcal{D}(\mathcal{U}_k)) = \frac{p(\boldsymbol{x}_k|\mathcal{Z}_{1:k-1})p(\mathcal{Z}_k|\boldsymbol{x}_k;\mathcal{D}(\mathcal{U}_k))}{\int p(\boldsymbol{x}_k|\mathcal{Z}_{1:k-1})p(\mathcal{Z}_k|\boldsymbol{x}_k;\mathcal{D}(\mathcal{U}_k))d\boldsymbol{x}_k}, \tag{20}$$

where $\mathcal{Z}_{1:k} = \{\mathcal{Z}_1, \mathcal{Z}_2, \ldots, \mathcal{Z}_k\}$ and

$$p(\boldsymbol{x}_k|\mathcal{Z}_{1:k-1}) = \int p(\boldsymbol{x}_k|\boldsymbol{x}_{k-1})p(\boldsymbol{x}_{k-1}|\mathcal{Z}_{1:k-1})d\boldsymbol{x}_{k-1}. \tag{21}$$

Note that (20) and (21) formulate the recursion of the posterior distribution $p(\boldsymbol{x}_k|\mathcal{Z}_{1:k};\mathcal{D}(\mathcal{U}_k))$ via the state transition probability $p(\boldsymbol{x}_k|\boldsymbol{x}_{k-1})$, the latest measurement model $p(\mathcal{Z}_k|\boldsymbol{x}_k;\mathcal{D}(\mathcal{U}_k))$ parametrized by $\mathcal{D}(\mathcal{U}_k)$, and the posterior distribution of the last step $p(\boldsymbol{x}_{k-1}|\mathcal{Z}_{1:k-1})$.

Here we give an example of the extended Kalman filter to clarify the formulations above. The extended Kalman filter gives the sufficient statistics (i.e., the posterior mean and error covariance matrix) to represent the assumed Gaussian posterior distribution $P(\boldsymbol{x}_k|\mathcal{Z}_{1:k};\mathcal{D}(\mathcal{U}_k))$ by linearizing the kinematic model and measurement model [57]. The complete recursion of the extended Kalman filter is given as,

$$\hat{\boldsymbol{x}}_{k|k-1} = \boldsymbol{f}_{k-1}(\hat{\boldsymbol{x}}_{k-1|k-1}), \tag{22}$$

$$P_{k|k-1} = F_{k-1}P_{k-1|k-1}F_{k-1}^{\mathsf{T}} + V_{k-1}, \tag{23}$$

$$K_k = P_{k|k-1}H_k^{\mathsf{T}}(H_kP_{k|k-1}H_k^{\mathsf{T}} + R_k)^{-1}, \tag{24}$$

$$\hat{\boldsymbol{x}}_{k|k} = \hat{\boldsymbol{x}}_{k|k-1} + K_k(\boldsymbol{z}_k - \boldsymbol{h}_k(\hat{\boldsymbol{x}}_{k|k-1};\mathcal{D}(\mathcal{U}_k))), \tag{25}$$

$$P_{k|k} = (I - K_kH_k)P_{k|k-1}, \tag{26}$$

where $\hat{\boldsymbol{x}}_{k|k-1}$ is the predicted state, $P_{k|k-1}$ is the corresponding predicted covariance matrix, $\hat{\boldsymbol{x}}_{k|k}$ is the updated state, and $P_{k|k}$ is the corresponding updated covariance matrix. Note that in the extended Kalman filter, $P(\boldsymbol{x}_k|\mathcal{Z}_{1:k-1})$ is assumed to be Gaussian with mean $\hat{\boldsymbol{x}}_{k|k-1}$ and covariance matrix $P_{k|k-1}$, and $P(\boldsymbol{x}_k|\mathcal{Z}_{1:k};\mathcal{D}(\mathcal{U}_k))$ is assumed to be Gaussian with mean $\hat{\boldsymbol{x}}_{k|k}$ and covariance matrix $P_{k|k}$. Furthermore, we have

$$F_{k-1} = \left.\frac{\partial \boldsymbol{f}_{k-1}(\boldsymbol{x})}{\partial \boldsymbol{x}^{\mathsf{T}}}\right|_{\boldsymbol{x}=\hat{\boldsymbol{x}}_{k-1|k-1}}, \tag{27}$$

$$H_k = \left.\frac{\partial \boldsymbol{h}_k(\boldsymbol{x};\mathcal{D}(\mathcal{U}_k))}{\partial \boldsymbol{x}^{\mathsf{T}}}\right|_{\boldsymbol{x}=\hat{\boldsymbol{x}}_{k|k-1}}. \tag{28}$$

Note that if noisy CV model is used, then F_{k-1} can be replaced by A_{k-1}.

2.5. Adaptive Tracking and Recursive Bayesian Estimation

In order to improve the tracking performance, we solve a combinatorial optimization problem for every tracking step after the measurements are received. According to the optimal solution, the radar network adaptively modifies its

geometry and assigns a subset of radars to collect measurements using the designed waveforms for the next step. In summary, the tracking procedure is iterated by alternating between the following two steps:

(1)
$$\mathcal{D}(\mathcal{U}_k) = \arg\max_{Q} \quad f(Q) \tag{29}$$
$$\text{s.t.} \quad \mathcal{U}_k^s \in \Pi_k(\mathcal{I}_k^s),$$
$$\mathcal{U}_k^p \in \mathcal{L}_k(\mathcal{U}_k^s, \mathcal{S}_{k-1}^p),$$

(2)
$$\hat{\boldsymbol{x}}_k = \arg\max_{\boldsymbol{x}_k} \quad P(\boldsymbol{x}_k|\mathcal{Z}_{1:k}; \mathcal{D}(\mathcal{U}_k)), \tag{30}$$

where $f(\cdot)$ is the utility function that evaluates the expected performance of the selected $\mathcal{D}(\mathcal{U}_k)$, $\mathcal{I}_k^s$ is set of the indices of radars that are available for management at time k, and $\Pi_k(\mathcal{I}_k^s)$ is the collection of the subsets of $\mathcal{I}_k^s$ according to a given policy. For example, $\Pi_k(\mathcal{I}_k^s) = \{\mathcal{U} \subset \mathcal{I}_k^s : |\mathcal{U}| \leq \tilde{c}\}$, where $\tilde{c}$ is a given constant, is commonly used in sensor selection. In addition, $\mathcal{S}_{k-1}^p$ denotes the states of all the radars in the sensor network at time $k-1$, and $\mathcal{L}_k(\mathcal{U}_k^s, \mathcal{S}_{k-1}^p)$ is the set of states (e.g., positions and velocities) that the selected radars can achieve at time k within the kinematic capabilities of the radars or as dictated by some predefined searching rules. For example, a radar may be responsible for exploring and monitoring a certain region, and unable to move far away from the initial position. Furthermore, the utility function $f(\cdot)$ can be one step ahead or multi-step ahead, depending on the demands and computational capacity.

As an illustrative example, an one-step ahead objective function could be the expected cross-entropy between the probability density functions (pdfs) of the predicted state and updated state, i.e.,

$$f(\mathcal{D}(\mathcal{U}_k)) = \mathbb{E}_{p(\boldsymbol{z}_k|\boldsymbol{x}_{k-1}=\hat{\boldsymbol{x}}_{k-1|k-1};\mathcal{D}(\mathcal{U}_k))}[-\mathbb{E}_{p(\boldsymbol{x}_k|\boldsymbol{z}_{1:k-1})} \log p(\boldsymbol{x}_k|\boldsymbol{z}_{1:k}; \mathcal{D}(\mathcal{U}_k)], \tag{31}$$

where the term in the square bracket is the cross-entropy, measuring the dissimilarity of the two pdfs. We need to take expectation of the cross-entropy with respect to $\boldsymbol{z}_k$ since $\boldsymbol{z}_k$ is not collected when solving the combinatorial optimization in (31). In order to compute the objective function, we can approximate $p(\boldsymbol{x}_k|\boldsymbol{z}_{1:k-1})$ and $p(\boldsymbol{x}_k|\boldsymbol{z}_{1:k}; \mathcal{D}(\mathcal{U}_k))$ using the output of the extended Kalman filter as suggested by (22)-(28), regardless of whether $\boldsymbol{z}_k$ includes some measurements containing only noise. For simplicity, the noisy CV model is used here. Also, note that

$$p(\boldsymbol{z}_k|\boldsymbol{x}_{k-1} = \hat{\boldsymbol{x}}_{k-1|k-1}; \mathcal{D}(\mathcal{U}_k)) = \int p(\boldsymbol{z}_k|\boldsymbol{x}_k; \mathcal{D}(\mathcal{U}_k)) p(\boldsymbol{x}_k|\boldsymbol{x}_{k-1} = \hat{\boldsymbol{x}}_{k-1|k-1}) d\boldsymbol{x}_k \tag{32}$$
$$\approx \sum_j p(\boldsymbol{z}_k|\tilde{\boldsymbol{x}}_k^j; \mathcal{D}(\mathcal{U}_k)) \frac{q(L(\tilde{\boldsymbol{x}}_k^j)|\boldsymbol{x}_{k-1} = \hat{\boldsymbol{x}}_{k-1|k-1})}{C} \tag{33}$$

where an approximation is used to remove the annoying integral in (32) to get (33) by discretizing the state $\boldsymbol{x}_k$ into 4-D grids with centers $\tilde{\boldsymbol{x}}_k^j$, and

$$q(L(\tilde{\boldsymbol{x}}_k^j)|\boldsymbol{x}_{k-1} = \hat{\boldsymbol{x}}_{k-1|k-1}) = \int_{L(\tilde{\boldsymbol{x}}_k^j)} p(\boldsymbol{x}_k|\boldsymbol{x}_{k-1} = \hat{\boldsymbol{x}}_{k-1|k-1}) d\boldsymbol{x}_k, \tag{34}$$

where $L(\tilde{\boldsymbol{x}}_k^j)$ is the grid that $\tilde{\boldsymbol{x}}_k^j$ locates, and C is the normalizing constant such that the summation of $q(L(\tilde{\boldsymbol{x}}_k^j)|\boldsymbol{x}_{k-1} = \hat{\boldsymbol{x}}_{k-1|k-1})$ is equal to 1. Furthermore, we can assume that the measurement collection processes of the selected radars

are independent (i.e., $E(\boldsymbol{n}_k^{(i)}\boldsymbol{n}_k^{(j)\mathsf{T}}) = R_k^{(i)}\delta_{ij}$), then

$$p(z_k|\tilde{\boldsymbol{x}}_k^j; \mathcal{D}(\mathcal{U}_k)) = \prod_{i\in\mathcal{U}_k^s} p(z_k^{(i)}|\tilde{\boldsymbol{x}}_k^j; D_k^{(i)}). \tag{35}$$

Note that $p(z_k^{(i)}|\tilde{\boldsymbol{x}}_k^j; D_k^{(i)})$ denotes the pdf of the measurement of i_{th} radar when the target state is given, and the expression is given as follows:

$$p(z_k^{(i)}|\tilde{\boldsymbol{x}}_k^j; D_k^{(i)}) = \begin{cases} p_{\boldsymbol{n}_k^{(i)}}(z_k^{(i)}) & \text{if scenario 1} \\ p_{\boldsymbol{n}_k^{(i)}}(z_k^{(i)} - \boldsymbol{h}_k^{(i)}(\tilde{\boldsymbol{x}}_k^j; D_k^{(i)})) & \text{if scenario 2} \end{cases},$$

where $p_{\boldsymbol{n}_k^{(i)}}(\cdot)$ is the pdf of the measurement noise $\boldsymbol{n}_k^{(i)}$. Note that the difference between the two scenarios:

- Scenario 1: The beam of radar i does not cover $\tilde{\boldsymbol{x}}_k^j$, and the measurement is only noise.
- Scenario 2: The beam of radar i covers $\tilde{\boldsymbol{x}}_k^j$, and the measurement is the echo from the target.

It follows that, we have that $z_k^{(i)}|\tilde{\boldsymbol{x}}_k^j \sim \mathcal{N}(\boldsymbol{\mu}^{(i)}(\tilde{\boldsymbol{x}}_k^j, D_k^{(i)}), R_k^{(i)})$, where

$$\boldsymbol{\mu}^{(i)}(\tilde{\boldsymbol{x}}_k^j, D_k^{(i)}) = \begin{cases} \mathbf{0} & \text{if scenario 1} \\ \boldsymbol{h}_k^{(i)}(\tilde{\boldsymbol{x}}_k^j; D_k^{(i)}) & \text{if scenario 2} \end{cases}. \tag{36}$$

Thus, we have $z_k|\tilde{\boldsymbol{x}}_k^j \sim \mathcal{N}(\boldsymbol{\mu}(\tilde{\boldsymbol{x}}_k^j, \mathcal{D}(\mathcal{U}_k)), R_k)$, where

$$\boldsymbol{\mu}(\tilde{\boldsymbol{x}}_k^j, \mathcal{D}(\mathcal{U}_k)) = \text{vec}\{\boldsymbol{\mu}^{(i)}(\tilde{\boldsymbol{x}}_k^j, D_k^{(i)})|i \in \mathcal{U}_k^s\}, \tag{37}$$

$$R_k = \text{diag}\{R_k^{(i)}|i \in \mathcal{U}_k^s\}, \tag{38}$$

where diag is the operator that rearranges the elements in the set into a block diagonal matrix.

Based on the above discussion and the extended Kalman filter, we can compute the cross-entropy as in (39) and have the explicit expression of the objective function in (40).

The state estimation shown by (30) is the maximum a posteriori (MAP) inference. Other estimators, such as the posterior mean, can also be selected if they fit better in the practical design. For the extended Kalman filter, the updated state shown by (25) is a good estimator.

2.6. Target Tracking with Multiple Target Models

Note that if the model of the complex reflectivity $\alpha(f_k^{(i)})$ with respect to $f_k^{(i)}$ is known by the sensing system, then the objective function like that in (40) can be directly applied. However, in many real applications, since the sensing system does not know the type of the target to track, it is unable to know how $f_k^{(i)}$ affects the complex reflectivity $\alpha(f_k^{(i)})$. In this paper, we assume that there exists a target model library, which includes multiple pre-trained target models. Note that each target model is associated with a mapping from the modulated frequency $f_k^{(i)}$ to $\alpha(f_k^{(i)})$. Formally, the target model library is given by

$$\mathcal{T} = \{\alpha_1(\cdot), \alpha_2(\cdot), \ldots, \alpha_M(\cdot)\}, \tag{41}$$

$$
\begin{aligned}
H_{\text{cross}} =& -\mathbb{E}_{p(\boldsymbol{x}_k|\boldsymbol{z}_{1:k-1})} \log p(\boldsymbol{x}_k|\boldsymbol{z}_{1:k}; \mathcal{D}(\mathcal{U}_k)) \\
=& \mathbb{E}_{p(\boldsymbol{x}_k|\boldsymbol{z}_{1:k-1})}[\frac{1}{2}\log(2\pi)^4 + \frac{1}{2}\log|P_{k|k}| + \frac{1}{2}(\boldsymbol{x}_k - \hat{\boldsymbol{x}}_{k|k})^\top P_{k|k}^{-1}(\boldsymbol{x}_k - \hat{\boldsymbol{x}}_{k|k})] \\
=& \frac{1}{2}\log(2\pi)^4 + \frac{1}{2}\log|P_{k|k}| + \frac{1}{2}\text{tr}(P_{k|k}^{-1}P_{k|k-1}) + \frac{1}{2}(\hat{\boldsymbol{x}}_{k|k} - \hat{\boldsymbol{x}}_{k|k-1})^\top P_{k|k}^{-1}(\hat{\boldsymbol{x}}_{k|k} - \hat{\boldsymbol{x}}_{k|k-1})]
\end{aligned} \tag{39}
$$

$$
\begin{aligned}
f(\mathcal{D}(\mathcal{U}_k)) =& \mathbb{E}_{p(\boldsymbol{z}_k|\boldsymbol{x}_{k-1}=\hat{\boldsymbol{x}}_{k-1|k-1};\mathcal{D}(\mathcal{U}_k))}[H_{\text{cross}}] \\
\approx& \frac{1}{2}\log(2\pi)^4 + \frac{1}{2}\log|P_{k|k}| + \frac{1}{2}\text{tr}(P_{k|k}^{-1}P_{k|k-1}) + \frac{1}{2}\text{tr}(K_k^\top P_{k|k}^{-1}K_k R_k) \\
&+ \frac{1}{2C}\sum_j [q(L(\tilde{\boldsymbol{x}}_k^j)|\boldsymbol{x}_{k-1} = \hat{\boldsymbol{x}}_{k-1|k-1})\times \\
&(\boldsymbol{\mu}(\tilde{\boldsymbol{x}}_k^j, \mathcal{D}(\mathcal{U}_k)) - \boldsymbol{h}_k(\hat{\boldsymbol{x}}_{k|k-1}))^\top K_k^\top P_{k|k}^{-1}K_k(\boldsymbol{\mu}(\tilde{\boldsymbol{x}}_k^j, \mathcal{D}(\mathcal{U}_k)) - \boldsymbol{h}_k(\hat{\boldsymbol{x}}_{k|k-1}))]
\end{aligned} \tag{40}
$$

---

where M is total number of the target models in the library. We assume that the actual target model is contained in the target model library. Now, we replace $f(\mathcal{D}(\mathcal{U}_k))$ with $f(\mathcal{D}(\mathcal{U}_k); \alpha_m)$ in order to emphasize the dependence of the objective function on the target model m. Then we have the modified objective function which will be applied to the combinatorial optimization problem in (29):

$$
\bar{f}(\mathcal{D}(\mathcal{U}_k)) = \frac{1}{M}\sum_{m=1}^{M} f(\mathcal{D}(\mathcal{U}_k); \alpha_m). \tag{42}
$$

Note that for simplicity, here we just average $f(\mathcal{D}(\mathcal{U}_k); \alpha_m)$ with respect to all the target models in the library by implicitly assuming the all the target models have the same probability of being correct at every tracking step. A more complicated strategy could be averaging the $f(\mathcal{D}(\mathcal{U}_k); \alpha_m)$ by assigning different weights to the target models in the library $\mathcal{T}$, and updating the weights at every step, using the information from consecutively received measurements.

Also, if the target model $\alpha(f_k^{(i)})$ is known in advance, then we can directly apply the recursive Bayesian state estimation to compute the posterior pdf $P(\boldsymbol{x}_k|\mathcal{Z}_{1:k}; \mathcal{D}(\mathcal{U}_k))$. If the actual target model is not available, then we need to average the the posterior pdf derived from a single target model m, denoted as $P_m(\boldsymbol{x}_k|\mathcal{Z}_{1:k}; \mathcal{D}(\mathcal{U}_k))$, on target models in the target model library.

Using the extended Kalman filter as an example, let the updated state and the corresponding covariance matrix with the m_{th} target model be denoted as $\boldsymbol{x}_{k|k,m}$ and $P_{k|k,m}$ respectively, and we have

$$
\hat{\boldsymbol{x}}_{k|k} = \frac{1}{M}\sum_{m=1}^{M} \hat{\boldsymbol{x}}_{k|k,m}, \tag{43}
$$

$$
P_{k|k} = \frac{1}{M}\sum_{m=1}^{M} \left(P_{k|k,m} + \hat{P}_{k,m}\right), \tag{44}
$$

where

$$\hat{P}_{k,m} = (\hat{\boldsymbol{x}}_{k|k,m} - \hat{\boldsymbol{x}}_{k|k})(\hat{\boldsymbol{x}}_{k|k,m} - \hat{\boldsymbol{x}}_{k|k})^{\mathsf{T}}. \tag{45}$$

Note that the above multiple model estimation also treats multiple target models having the same possibility as the actual model, as what we do when dealing with the objective function. More complicated multiple model estimation methods could be employed [57].

The sketch of the target tracking procedure is described as algorithm 1. In general, nested loops are needed to exhaustively search for the optimal solution of a combinatorial optimization problem at every step. In practical applications, it is realistic to select the same or nearly the same waveform parameters between consecutive dwells (steps) separated by a very short time period, such that the computational complexity can be reduced on average. Furthermore, the objective function of the optimization problem can be carefully designed with some good properties, e.g., submodularity. In this way, some greedy methods can be applied to solve the combinatorial optimization problem with guaranteed performance.

Algorithm 1: Target Tracking in a Network of Radars

Input : Initial pdf of the target state $p(\boldsymbol{x}_0)$, and initial radars' state S_0^p

Output: The optimal set $\hat{\mathcal{D}}(\mathcal{U}_k)$, the posterior pdf $P(\boldsymbol{x}_k|\mathcal{Z}_{1:k}; \mathcal{D}(\mathcal{U}_k))$, and MAP inference $\hat{\boldsymbol{x}}$

```
k ← 1;
while Stop condition is not met do
    for each target model m do
        for each subset of radars U_k^s ∈ Π_k(I_k^s) do
            for states of radars U_k^p ∈ L_k(U_k^s, S_{k-1}^p) do
                for waveforms of radars U_k^w do
                    Compute f(D(U_k); α_m);
    Compute the objective function f̄(D(U_k));
    Search the solution D̂(U_k) = arg max f̄(D(U_k));
    Get the measurement z_k by the setting D̂(U_k);
    for each target model m do
        Get P_m(x_k|Z_{1:k}; D̂(U_k)) using recursive Bayesian state estimation;
    Average on the target model to get the posterior pdf P(x_k|Z_{1:k}; D̂(U_k));
    Update radars' state S_k^p by a predefined rule for the radars that are not selected;
    k ← k + 1;
```

3. Simulation Results

The framework given by Section 2 is general, which would fit many tracking applications in the sensor network, and numerical simulations are needed to demonstrate the framework. In this section, an illustrative example is discussed in order to formulate a specific scenario as shown in Figure 2. The Figure 2 illustrates a network with small number of radars for the sake of simple illustration; however it represents a scenario with large-scale network of cognitive radars which have certain constraints about coverage area and path. Especially, assuming that each radar in the network is aware of the location of the other radars in the network and also assuming that the target is in the far-field compared to all the radars in the network, the scenario presents here a realistic case in which the overlap among the radars along the same path is avoided. Moreover, without loss of generality, the paths are assumed to be along the x and y axes in Figure 2; however, in general these radar paths could be rotated. Based on this scenario, a simulation-based validation demonstrates the feasibility of the proposed method.

3.1. Simulation Settings (a Scenario)

As shown in Fig. 2, a total of J_{total} radars are moving along the x and y axes to track a single target in a 2-D plane. A central processing system fuses the measurements from all the operative radars and manages the network by dictating the waveform design, path planning, and radar selection. In order to simplify the case, we make the following assumption for this illustrative example.

- All the radars that move in the same direction transmit waveforms with the same range resolution by using the waveforms given by the specific example in Section 2.1. Thus, the 2-D plane can be divided into several lattices. Each lattice has the size $\delta x \times \delta y$, where δx and δy are the range resolutions of the waveforms transmitted by the radars moving on the y and x axes, respectively.

- At every tracking step, each radar is located only at the discrete coordinates on x and y axes corresponding to the centers of rows and columns formed by lattices.

- Each radar is able to emit a signal only in the direction orthogonal to its moving direction. For example, radar x_i can emit a signal only in y direction.

- The beamwidths of the radars are considered to cover only one column or one row. For example, if a radar is moving in the x direction, its beam covers only one column of lattices if it is selected to operate.

- The target is moving in the far field, which is a common scenario in practice. Since the beamwidth of a radar is comparable to its range resolution in this case, for the echo from the target, we can approximate the time delay and Doppler frequency in simper expressions. In other words, if i_{th} radar on the x axis receives the echo from the target, we can approximate (3) and (4) as

$$\tau^{(i)} \approx \frac{2y}{c}, \qquad \nu^{(i)} \approx -\frac{2f_c\dot{y}}{c}, \tag{46}$$

where the approximation is due to that the far field assumption results in $|x - x^{(i)}| \ll |y - y^{(i)}| = |y|$ for the i_{th} radar on the x axis. A similar approximation can be applied to radars on the y axis. We emphasize that the time delay and Doppler frequency of the echo from the target are not functions of the position or velocity of the radar if it receives the echo.

- In addition, since we have multiple radars moving on the each axis, we let each radar have its own predefined assigned surveillance space which consists of contiguous columns or rows, and the surveillance spaces of different radars are not overlapped if they are moving in the same direction. Also, the union of the assigned surveillance regions of the radars moving in the same direction covers the whole workspace of interest. In this example, we assign each radar in the network the responsibility of monitoring 3 consecutive columns or rows in the space. The centers of the assigned surveillance regions of radar x_1 and y_1 correspond to the lattice that initial state $\hat{\boldsymbol{x}}_{0|0}$ locates. In order to reduce the searching complexity of solving the combinatorial optimization problem, at each time k, only 5 columns or rows near the predicted state $\hat{\boldsymbol{x}}_{k+1|k}$ and the corresponding radars are considered.

- Target remains in only one lattice during the time when the measurements of a tracking step are collected.

- Radar measurement collection procedures are independent; i.e., the measurement of one radar is not affected by signals emitted by other radars and is independent of the measurements of other radars.

- The power of the measurement noise of each radar is assumed to be known in advance, and the environment is assumed to be stationary.

In summary, each radar is responsible for a predefined surveillance region, and it transmits a signal covering one column or one row of the lattices in its region if it is selected by the central processing system to operate.

In this illustrative example, we let the target start with a state sampled from a Gaussian distribution $\mathcal{N}(\hat{\boldsymbol{x}}_{0|0}, P_{0|0})$, where $\hat{\boldsymbol{x}}_{0|0} = [630\text{ m},\ 150\text{ m/s},\ 630\text{ m},\ 150\text{ m/s}]^{\mathsf{T}}$ and $P_{0|0} = \text{diag}(1, 0.01, 1, 0.01)$. For the signal model shared by all the radars in the network, we set $u(t)$ in (5) as a square pulse, with pulse width $t_{\text{width}} = 10^{-7}$ s and power 1. The carrier frequency is $f_c = 3$ GHz, and the modulated frequency $f_c + f_\xi^{(i)}$ can be selected from $[f_c - (1\text{ MHz}),\ f_c,\ f_c + (1\text{ MHz})]^{\mathsf{T}}$ in every tracking step. In addition, the speed of light $c = 3 \times 10^8$ m/s, and the range resolutions can be computed as $\delta x = \delta y = c \times t_{\text{width}}/2 = 15$ m. We adopt the noisy constant velocity (CV) model suggested by (7) as the underlying kinematic model, where the interval between two tracking steps is $T_{\text{in}} = 0.005$ s or 0.05 s, which varies in the different experiments. The process noise intensities, q_1 and q_2, vary in the different experiments. Also, we use the raw discretized signals received from the selected radars as the measurements, and the corresponding measurement model is given by (18). In this model, the sampling frequency is $f_s = 20$ MHz. We take the first 334 sample points as the measurement vector in the experiments. The power of the measurement noise is $\mathbb{E}[n_k^{(i)}(t_p) n_k^{(i)}(t_q)^*] = 0.02\delta_{pq}$ for all time k and radar i, where t_p and t_q correspond to the time of two sample points. We use the extended Kalman filter to do the recursive Baysian state estimation, as stated in Section 2.4.

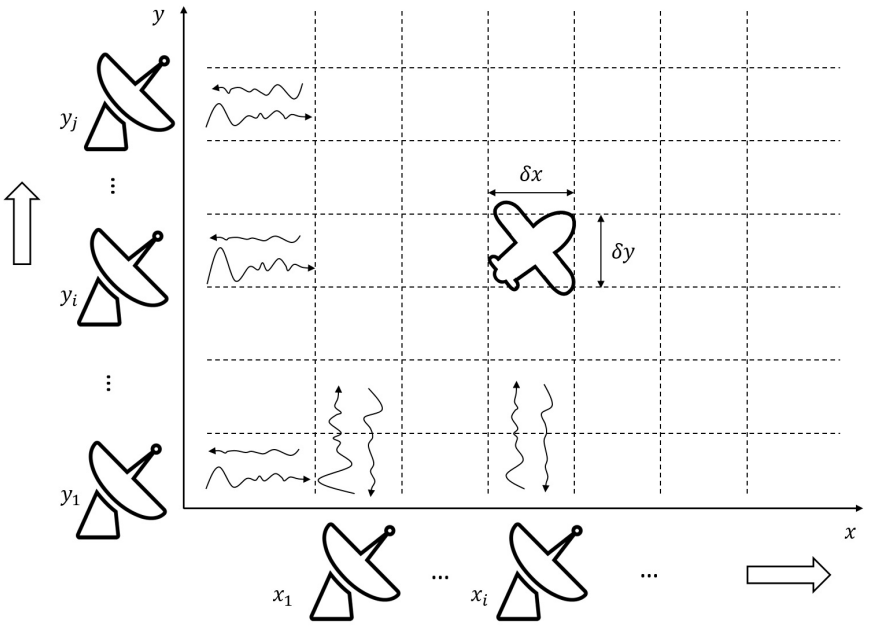

Figure 2: Model settings of the illustrative example of the framework.

The objective function of the combinatorial optimization problem in (29) could be given by the expected cross-entropy, where the definition is shown in (31), and the analytical expression is given by (40). Note that in Section 2.5, we approximate the integral in (32) with a summation by discretizing the state space of $\boldsymbol{x}_k$ into 4-D grids. Here, we discretize only the position of the state space and fix the velocity of $\boldsymbol{x}_k$ as the predicted velocity of $\hat{\boldsymbol{x}}_{k|k-1}$ in order to reduce the computational complexity. The feasible set for the sensor selection within the constraints of (29) is defined as

$$\Pi_k(\mathcal{I}_k^s) = \{\mathcal{U} \subset \mathcal{I}_k^s : |\mathcal{U}| = 2, \text{ and two radars are moving on the } x \text{ and } y \text{ axes respectively}\}, \tag{47}$$

which means that for each axis, we select one radar to get the measurements. This is a reasonable policy since the assigned surveillance regions are not overlapped for radars that move in the same direction. Based on this policy, $\mathcal{U}_k^s$ can be expressed by $(x_{i,k}, y_{j,k})$, where $x_{i,k}$ and $y_{j,k}$ are two indices of radars moving on the x and y axes respectively. For the path planning constraints $\mathcal{U}_k^p \in \mathcal{L}_k(\mathcal{U}_k^s, \mathcal{S}_{k-1}^p)$, we additionally assume that each radar is capable of transmitting the signal to any column or row in its assigned surveillance region at any step. In other words, each radar can move fast enough between any two tracking steps in its assigned range. In this example, the path planning constraint $\mathcal{U}_k^p \in \mathcal{L}_k(\mathcal{U}_k^s, \mathcal{S}_{k-1}^p)$ dictates that radars do not leave the ranges corresponding to their assigned surveillance regions. Furthermore, we do not need to take the velocities of sensors into account when solving the combinatorial optimization problem, since they do not affect the objective function and the path planning constraint. Moreover, multiple target models, as shown in Section 2.6, are considered in this example. We assume that there are three target models in the target model library $\{\alpha_m(f_\xi) : m = 1, 2, 3\}$. Specifically, they are $\alpha_1(\{-1, 0, 1\}) = \{1/\sqrt{21},\ 2/\sqrt{21},\ 4/\sqrt{21}\}$,

Algorithm 2: Target Tracking in the illustrative example

Input : Initial State $\hat{\boldsymbol{x}}_{0|0}$ and Covariance Matrix $P_{0|0}$

Output: Selected radar pair $(x_{i,k}, y_{j,k})$, radar waveforms $(f_{\xi,k}^{w_x}, f_{\xi,k}^{w_y})$, and the radar positions $(r^{p_x}(x_{i,k}), r^{p_y}(y_{j,k}))$ in the ranges of the assigned surveillance regions at every step k. The updated state $\hat{\boldsymbol{x}}_{k|k}$ and covariance matrix $P_{k|k}$.

```
k ← 1;
while Stop condition is not met do
    for each target model m do
        for each radar pair do
            for each position pair in the ranges of the assigned regions of the selected radar pair do
                for each waveform pair do
                    Compute f(D(U_k); α_m);
    Compute the objective function f̄(D(U_k));
    Search the solution D̂(U_k) = arg max f̄(D(U_k));
    Get the measurement z_k by the setting D̂(U_k);
    for each target model m do
        Get x̂_{k|k,m} and P_{k|k,m} using the extended Kalman filter;
    Average on the target model to get x̂_{k|k} and P_{k|k};
    k ← k + 1;
```

$\alpha_2(\{-1, 0, 1\}) = \{2/\sqrt{9}, 1/\sqrt{9}, 2/\sqrt{9}\}$, and $\alpha_3(\{-1, 0, 1\}) = \{1/\sqrt{14}, 2/\sqrt{14}, 3/\sqrt{14}\}$. In the simulation, we use the first target model α_1 as the underlying target model, which is not known by the sensor system.

In summary, the sketch of the target tracking procedure in this illustrative example can be described as algorithm 2.

3.2. Simulation Results

All the experiments conduct 60 tracking steps, and all the relative errors are computed using 30 Monte Carlo runs in this section. The performance of the framework on the illustrative example is illustrated in Fig. 3, Fig. 4, and Fig. 5. Fig. 3 shows the performance of the tracking procedure with process noise intensities $q_1 = q_2 = 0.1$ and the tracking time interval $T_{\text{in}} = 0.005$ s. Fig. 3(a) shows a representative example of the true trajectory and estimated trajectory. Fig. 3(b)-3(e) show the relative errors of the positions and velocities of the updated state. Fig. 3(f) shows the waveforms used by the radars on the x and y axes in the representative example. Fig. 4 shows the corresponding performance with $q_1 = q_2 = 0.1$ and $T_{\text{in}} = 0.05$ s. We can see from the results that the proposed framework is capable

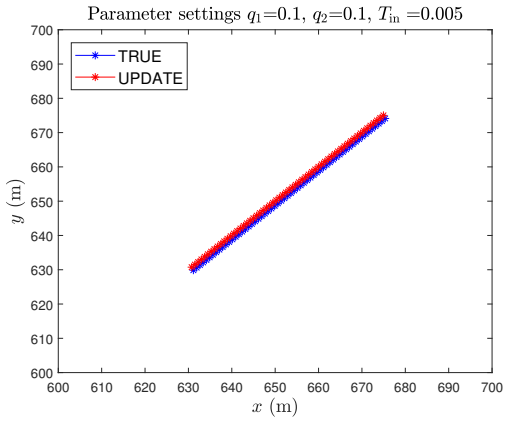

(a) The true and estimated trajectories

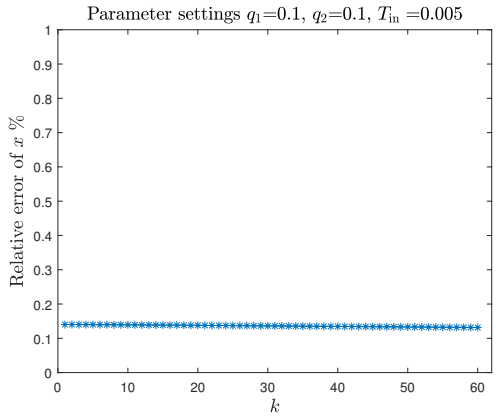

(b) Relative error of x

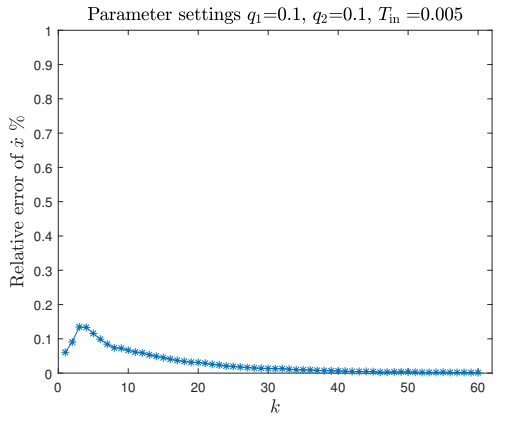

(c) Relative error of $\dot{x}$

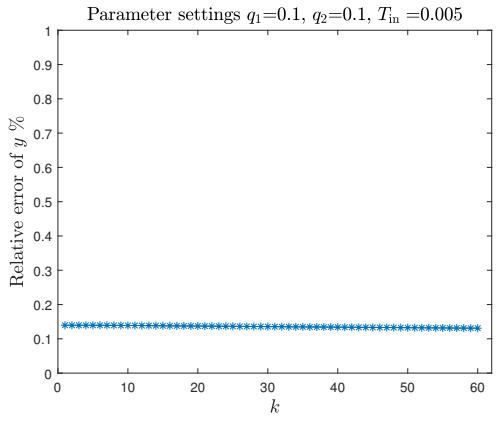

(d) Relative error of y

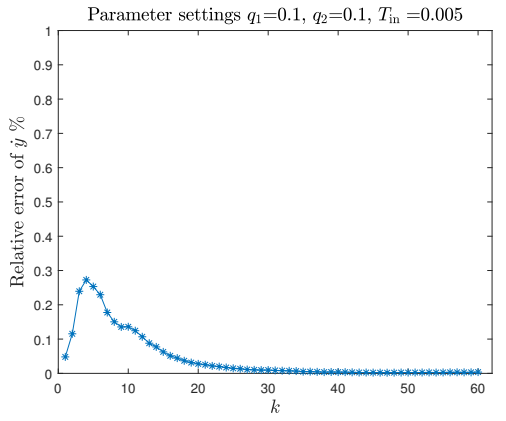

(e) Relative error of $\dot{y}$

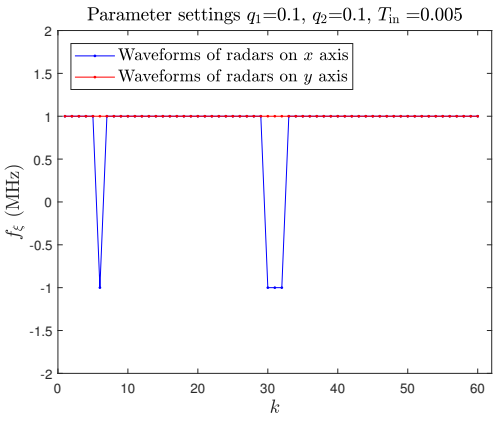

(f) Waveforms used by radars

Figure 3: Tracking performance when process noise intensities $q_1 = q_2 = 0.1$, and the tracking time interval $T_{\text{in}} = 0.005$ s. (a) Comparison of the true and estimated trajectories of the target, (b) relative error of the position x, (c) relative error of the velocity $\dot{x}$, (d) relative error of the position y, (e) relative error of the velocity $\dot{y}$, (f) waveforms used by radars on the x and y.

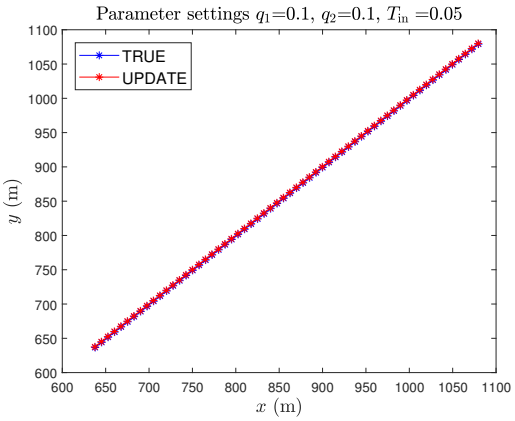

(a) The true and estimated trajectories

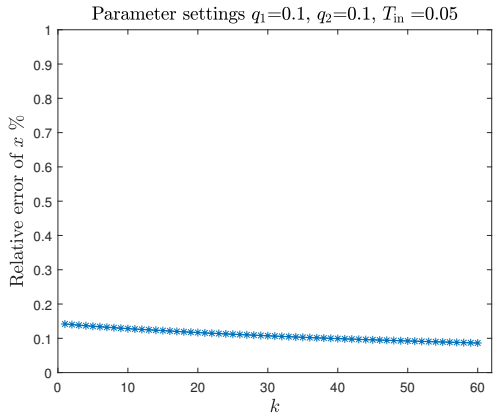

(b) Relative error of x

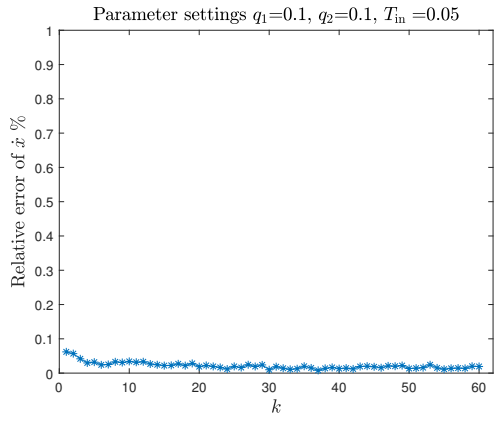

(c) Relative error of $\dot{x}$

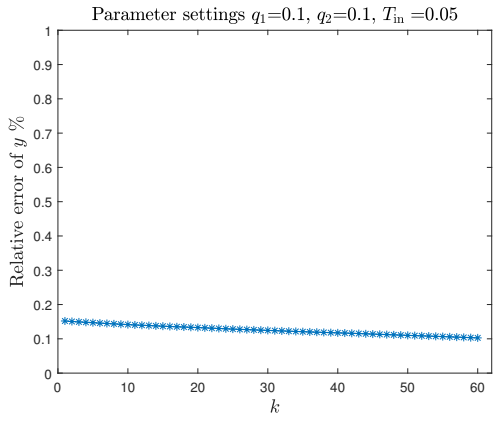

(d) Relative error of y

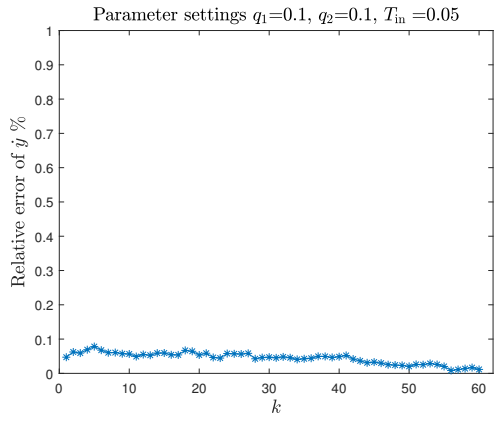

(e) Relative error of $\dot{y}$

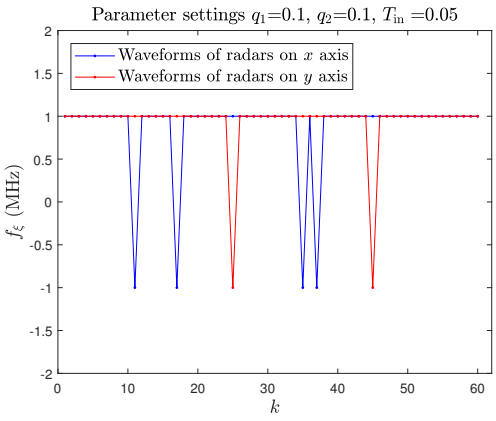

(f) Waveforms used by radars

Figure 4: Tracking performance when process noise intensities $q_1 = q_2 = 0.1$, and the tracking time interval $T_{\text{in}} = 0.05$ s. (a) Comparison of the true and estimated trajectories of the target, (b) relative error of the position x, (c) relative error of the velocity $\dot{x}$, (d) relative error of the position y, (e) relative error of the velocity $\dot{y}$, (f) waveforms used by radars on the x and y.

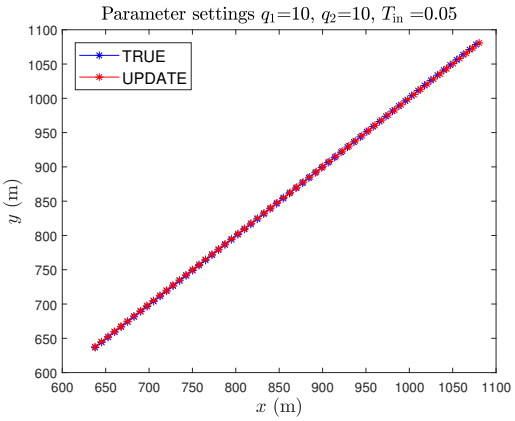

(a) The true and estimated trajectories

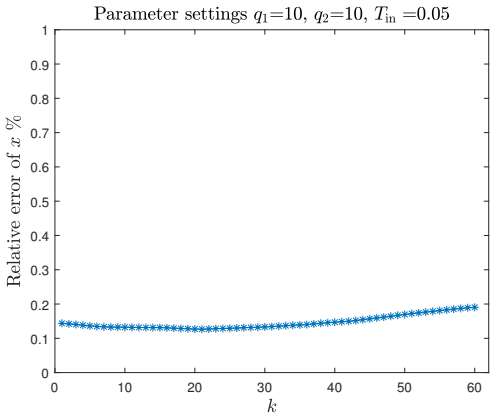

(b) Relative error of x

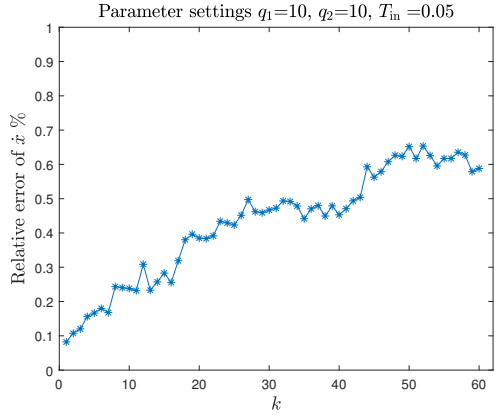

(c) Relative error of $\dot{x}$

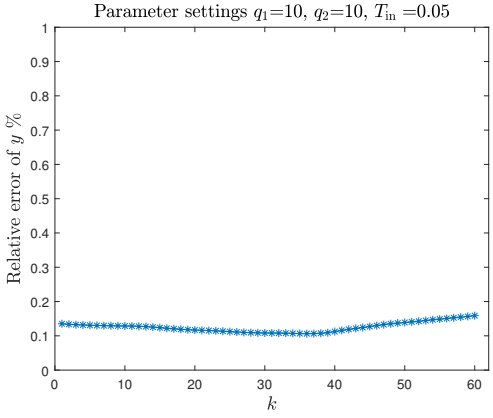

(d) Relative error of y

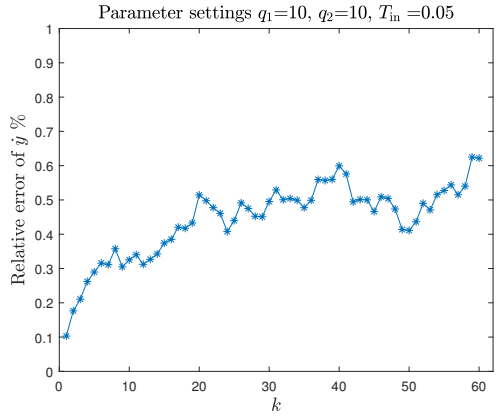

(e) Relative error of $\dot{y}$

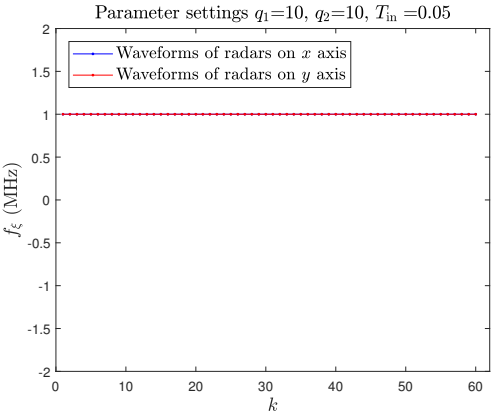

(f) Waveforms used by radars

Figure 5: Tracking performance when process noise intensities $q_1 = q_2 = 10$, and the tracking time interval $T_{\text{in}} = 0.05$ s. (a) Comparison of the true and estimated trajectories of the target, (b) relative error of the position x, (c) relative error of the velocity $\dot{x}$, (d) relative error of the position y, (e) relative error of the velocity $\dot{y}$, (f) waveforms used by radars on the x and y.

of tracking a single target in the sensor network under these two sets of parameters. From the representative examples of the trajectories, we note that the estimated states are close to the true states, which is also verified by the behaviors of the relative errors. We also notice that when the tracking time interval T_{in} (i.e., pulse repetition interval (PRI) in this example), is relatively small, further decreasing it could provide better velocity tracking performance after the algorithm converges, by comparing relative errors of velocities $\dot{x}$ and $\dot{y}$ in Fig. 3 and Fig. 4. Note that shorter PRI usually requires the higher power usage, and longer tracking time interval means higher uncertainty of the target state between two tracking steps, thus hindering the tracking performance. Hence, in practical use, the sensor network should utilize the freedom of choosing an appropriate PRI to balance the power usage and tracking performance, or adaptively adjust the PRI to address different scenarios.

When the process noise intensities become larger, which is shown by Fig. 5 with $q_1 = q_2 = 10$ and $T_{\text{in}} = 0.05$ s, the relative errors increase as tracking time moves on, especially the relative errors of the velocities. This is in accordance with the intuition, since when process noise intensities are larger, the motion of the target becomes more unpredictable. In addition, the extended Kalman filter is a sub-optimal tracking filter and the errors caused by linearization accumulate, resulting in such a scenario. Note that the simulation generates the true state using this noisy CV kinematic model. In practice, the target maneuvers by switching itself among several predefined motion modes, such as constant velocity mode, accelerating mode, and turning mode. Thus, the noisy CV kinematic model with large process intensities might not be a real case for target's motion, and multiple model-based tracking filters, such as the interacting multiple model (IMM) filter, are needed to address practical situations.

The waveforms used by the radars moving on x and y axes are shown in Fig. 3(f), 4(f), and 5(f) for these three sets of parameters. Note that for all the three cases, the radars prefer to use the frequency $f_\xi + f_c = f_c + (1 \text{ MHz})$. Note that the underlying true target model is $\alpha_1(\{-1, 0, 1\}) = \{1/\sqrt{21}, 2/\sqrt{21}, 4/\sqrt{21}\}$. Thus, the radars tend to use the frequencies corresponding to highest signal-to-noise ratio (SNR), such that more information can be collected from the measurements to maximize the objective function. Moreover, we need to claim that the waveform design is also affected by the target model library. In this example, we assume that all the target models in the library have the same probabilities to be correct along the whole tracking time, and we can see that all the target models in the library suggest that $f_\xi + f_c = f_c + (1 \text{ MHz})$ corresponds to highest SNR. In practice, we may need to update the probability of each target model by utilizing the received measurements.

4. Conclusion

In this paper, we proposed a framework of single target tracking in a cognitive network of radars, jointly considering waveform design, path planning, and radar selection. We applied theories of DGM and RBSE to formulate the framework, which consists of alternately solving the combinatorial optimization problem and estimating the target state. In addition, the framework was demonstrated by an illustrative example and verified by numerical simulations. We emphasize that the proposed framework is not limited to the illustrative example, and could be applied to much

more complicated scenarios. In this paper, we only used a grid search method to solve the combinatorial optimization problem to get the optimal waveforms, radar locations, and operating radars. More precisely, 5×5 grids near the expected state were searched in the optimization to find the optimal solution in each step. Waveform parameters can be shared among consecutive dwells separated by a short time period to further reduce the average computational complexity. An objective function with some particular properties, e.g., submodularity, can also be designed to be compatible with greedy methods. Note that only the expected cross-entropy was considered as the objective function to explore the environment. Moreover, objective functions that can explore the environment and exploit the current knowledge could be taken into account, and multi-objective optimization technique can be applied to combine the exploration and exploitation. In addition, the environmental model deserves further investigation to include geography information and waveform-dependent clutters, so that a more practical radar network management strategy can be developed.

References

[1] S. Haykin, Cognitive radar: A way of the future, IEEE signal processing magazine 23 (1) (2006) 30–40.

[2] K. L. Bell, C. J. Baker, G. E. Smith, J. T. Johnson, M. Rangaswamy, Cognitive radar framework for target detection and tracking, IEEE Journal of Selected Topics in Signal Processing 9 (8) (2015) 1427–1439.

[3] A. O. Hero, D. Cochran, Sensor management: Past, present, and future, IEEE Sensors Journal 11 (12) (2011) 3064–3075.

[4] S. Kay, Optimal signal design for detection of Gaussian point targets in stationary Gaussian clutter/reverberation, IEEE journal of selected topics in signal processing 1 (1) (2007) 31–41.

[5] S. Kay, Waveform design for multistatic radar detection, IEEE Transactions on Aerospace and Electronic Systems 45 (3).

[6] X.-b. Deng, C.-y. Qiu, Z. Cao, M. Morelande, B. Moran, Waveform design for enhanced detection of extended target in signal-dependent interference, IET Radar, Sonar & Navigation 6 (1) (2012) 30–38.

[7] S. Sen, A. Nehorai, Adaptive OFDM radar for target detection in multipath scenarios, IEEE Transactions on Signal Processing 59 (1) (2011) 78–90.

[8] S. Sen, G. Tang, A. Nehorai, Multiobjective optimization of OFDM radar waveform for target detection, IEEE Transactions on Signal Processing 59 (2) (2011) 639–652.

[9] M. Hurtado, A. Nehorai, Polarimetric detection of targets in heavy inhomogeneous clutter, IEEE Transactions on Signal Processing 56 (4) (2008) 1349–1361.

[10] S. Sen, Characterizations of PAPR-constrained radar waveforms for optimal target detection, IEEE Sensors Journal 14 (5) (2014) 1647–1654.

[11] M. Hurtado, T. Zhao, A. Nehorai, Adaptive polarized waveform design for target tracking based on sequential Bayesian inference, IEEE Transactions on Signal Processing 56 (3) (2008) 1120–1133.

[12] S. Sen, A. Nehorai, OFDM MIMO radar with mutual-information waveform design for low-grazing angle tracking, IEEE Transactions on Signal Processing 58 (6) (2010) 3152–3162.

[13] S.-M. Hong, R. J. Evans, H.-S. Shin, Control of waveforms and detection thresholds for optimal target tracking in clutter, in: Proceedings of the 39th IEEE Conference on Decision and Control (CDC), Vol. 4, 2000, pp. 3906–3907.

[14] S.-M. Hong, R. J. Evans, H.-S. Shin, Optimization of waveform and detection threshold for range and range-rate tracking in clutter, IEEE Transactions on Aerospace and Electronic Systems 41 (1) (2005) 17–33.

[15] D. J. Kershaw, R. J. Evans, Optimal waveform selection for tracking systems, IEEE Transactions on Information Theory 40 (5) (1994) 1536–1550.

[16] D. J. Kershaw, R. J. Evans, Waveform selective probabilistic data association, IEEE Transactions on Aerospace and Electronic Systems 33 (4) (1997) 1180–1188.

[17] C. Rago, P. Willett, Y. Bar-Shalom, Detection-tracking performance with combined waveforms, IEEE Transactions on Aerospace and Electronic Systems 34 (2) (1998) 612–624.

[18] R. Niu, P. Willett, Y. Bar-Shalom, Tracking considerations in selection of radar waveform for range and range-rate measurements, IEEE Transactions on Aerospace and Electronic Systems 38 (2) (2002) 467–487.

[19] D. Cochran, S. Suvorova, S. D. Howard, B. Moran, Waveform libraries, IEEE Signal Processing Magazine 26 (1) (2009) 12–21.

[20] S. P. Sira, A. Papandreou-Suppappola, D. Morrell, Dynamic configuration of time-varying waveforms for agile sensing and tracking in clutter, IEEE Transactions on Signal Processing 55 (7) (2007) 3207–3217.

[21] J. Zhang, B. Manjunath, G. Maalouli, A. Papandreou-Suppappola, D. Morrell, Dynamic waveform design for target tracking using MIMO radar, in: 42nd Asilomar Conference on Signals, Systems and Computers (ASILOMAR), 2008, pp. 31–35.

[22] C. O. Savage, B. Moran, Waveform selection for maneuvering targets within an IMM framework, IEEE Transactions on Aerospace and Electronic Systems 43 (3).

[23] M. Hurtado, J.-J. Xiao, A. Nehorai, Target estimation, detection, and tracking, IEEE Signal Processing Magazine 26 (1) (2009) 42–52.

[24] M. Hurtado, A. Nehorai, Bat-inspired adaptive design of waveform and trajectory for radar, in: 42nd Asilomar Conference on Signals, Systems and Computers (ASILOMAR), 2008, pp. 36–40.

[25] R. McAulay, J. Johnson, Optimal mismatched filter design for radar ranging, detection, and resolution, IEEE Transactions on Information Theory 17 (6) (1971) 696–701.

[26] S. P. Sira, Y. Li, A. Papandreou-Suppappola, D. Morrell, D. Cochran, M. Rangaswamy, Waveform-agile sensing for tracking, IEEE Signal Processing Magazine 26 (1) (2009) 53–64.

[27] P. Tichavsky, C. H. Muravchik, A. Nehorai, Posterior Cramér-Rao bounds for discrete-time nonlinear filtering, IEEE Transactions on signal processing 46 (5) (1998) 1386–1396.

[28] T. M. Cover, J. A. Thomas, Elements of information theory, John Wiley & Sons, 2012.

[29] S. Suvorova, S. Howard, W. Moran, R. Evans, Waveform libraries for radar tracking applications: Maneuvering targets, in: 40th Annual Conference on Information Sciences and Systems (CISS), 2006, pp. 1424–1428.

[30] S. Suvorova, D. Musicki, B. Moran, S. Howard, B. La Scala, Multi step ahead beam and waveform scheduling for tracking of manoeuvering targets in clutter, in: IEEE International Conference on Acoustics, Speech, and Signal Processing (ICASSP), Vol. 5, 2005, pp. v–889.

[31] M. R. Bell, Information theory and radar waveform design, IEEE Transactions on Information Theory 39 (5) (1993) 1578–1597.

[32] N. H. Nguyen, K. Dogancay, L. M. Davis, Adaptive waveform selection for multistatic target tracking, IEEE Transactions on Aerospace and Electronic Systems 51 (1) (2015) 688–701.

[33] D. Cochran, Waveform-agile sensing: opportunities and challenges, in: IEEE International Conference on Acoustics, Speech, and Signal Processing (ICASSP), Vol. 5, 2005, pp. v–877.

[34] K. Dogancay, UAV path planning for passive emitter localization, IEEE Transactions on Aerospace and Electronic systems 48 (2) (2012) 1150–1166.

[35] K. Dogancay, Single-and multi-platform constrained sensor path optimization for angle-of-arrival target tracking, in: 18th European Signal Processing Conference (EUSIPCO), 2010, pp. 835–839.

[36] Y. Oshman, P. Davidson, Optimization of observer trajectories for bearings-only target localization, IEEE Transactions on Aerospace and Electronic Systems 35 (3) (1999) 892–902.

[37] K. Zhou, S. I. Roumeliotis, Optimal motion strategies for range-only constrained multisensor target tracking, IEEE Transactions on Robotics 24 (5) (2008) 1168–1185.

[38] B. Grocholsky, A. Makarenko, H. Durrant-Whyte, Information-theoretic coordinated control of multiple sensor platforms, in: IEEE International Conference on Robotics and Automation (ICRA), Vol. 1, 2003, pp. 1521–1526.

[39] N. H. Nguyen, K. Doğançay, Optimal sensor placement for Doppler shift target localization, in: IEEE Radar Conference (RadarCon), 2015,

pp. 1677–1682.

[40] S. Joshi, S. Boyd, Sensor selection via convex optimization, IEEE Transactions on Signal Processing 57 (2) (2009) 451–462.

[41] M. Shamaiah, S. Banerjee, H. Vikalo, Greedy sensor selection: Leveraging submodularity, in: 49th IEEE Conference on Decision and Control (CDC), 2010, pp. 2572–2577.

[42] X. Shen, P. K. Varshney, Sensor selection based on generalized information gain for target tracking in large sensor networks, IEEE Transactions on Signal Processing 62 (2) (2014) 363–375.

[43] A. S. Narykov, O. A. Krasnov, A. Yarovoy, Algorithm for resource management of multiple phased array radars for target tracking, in: Proceedings of the 16th International Conference on Information Fusion (ISIF), 2013, pp. 1258–1264.

[44] A. S. Narykov, A. Yarovoy, Sensor selection algorithm for optimal management of the tracking capability in multisensor radar system, in: 2013 European Microwave Conference (EuMC), 2013, pp. 1811–1814.

[45] M. Xie, W. Yi, L. Kong, Joint node selection and power allocation for multitarget tracking in decentralized radar networks, in: 19th International Conference on Information Fusion (FUSION), 2016, pp. 45–52.

[46] P. Chavali, A. Nehorai, Scheduling and power allocation in a cognitive radar network for multiple-target tracking, IEEE Transactions on Signal Processing 60 (2) (2012) 715–729.

[47] H. Godrich, A. Petropulu, H. V. Poor, Cluster allocation schemes for target tracking in multiple radar architecture, in: Conference Record of the Forty Fifth Asilomar Conference on Signals, Systems and Computers (ASILOMAR), 2011, pp. 863–867.

[48] A. S. Chhetri, D. Morrell, A. Papandreou-Suppappola, Scheduling multiple sensors using particle filters in target tracking, in: IEEE Workshop on Statistical Signal Processing (SSP), 2003, pp. 549–552.

[49] N. Cao, S. Choi, E. Masazade, P. K. Varshney, Sensor selection for target tracking in wireless sensor networks with uncertainty, IEEE Transactions on Signal Processing 64 (20) (2016) 5191–5204.

[50] N. H. Nguyen, K. Dogancay, L. M. Davis, Joint transmitter waveform and receiver path optimization for target tracking by multistatic radar system, in: IEEE Workshop on Statistical Signal Processing (SSP), 2014, pp. 444–447.

[51] B. Manjunath, J. J. Zhang, A. Papandreou-Suppappola, D. Morrell, Sensor scheduling with waveform design for dynamic target tracking using MIMO radar, in: Conference Record of the Forty-Third Asilomar Conference on Signals, Systems and Computers (ASILOMAR), 2009, pp. 141–145.

[52] N. H. Nguyen, K. Doğançay, L. M. Davis, Adaptive waveform and Cartesian estimate selection for multistatic target tracking, Signal Processing 111 (2015) 13–25.

[53] Y. Xiang, M. Akcakaya, S. Sen, D. Erdogmus, A. Nehorai, Target tracking via recursive bayesian state estimation in radar networks, in: 51st Asilomar Conference on Signals, Systems, and Computers, 2017, pp. 880–884.

[54] J. Geweke, H. Tanizaki, Bayesian estimation of state-space models using the Metropolis-Hastings algorithm within Gibbs sampling, Computational Statistics and Data Analysis 37 (2) (2001) 151 – 170.

[55] N. J. Gordon, D. J. Salmond, A. F. M. Smith, Novel approach to nonlinear/non-Gaussian Bayesian state estimation, IEE Proceedings F - Radar and Signal Processing 140 (2) (1993) 107–113.

[56] Y. Bar-Shalom, X. R. Li, T. Kirubarajan, Estimation with applications to tracking and navigation: theory algorithms and software, John Wiley & Sons, 2004.

[57] C.-B. Chang, K.-P. Dunn, Applied State Estimation and Association, MIT Press, 2016.